

Mode Combining Components in Multimode MIMO Transmission Systems

Steffen Lochmann¹, Andreas Ahrens²

Hochschule Wismar, University of Technology, Business and Design,
Philipp-Müller-Straße 14, 23966 Wismar, Germany

¹steffen.lochmann@hs-wismar.de, ²andreas.ahrens@hs-wismar.de

Abstract

The concept of MIMO (multiple input multiple output) transmission over multimode fibers has attracted increasing interest within the last years. Theoretically, the performance of the optical MIMO multimode channel is well predictable. However, the realization of the optical MIMO channel requires substantial further research. In this work the efficiency of optical couplers in MIMO systems is studied in a 1,4 km multimode testbed. Optical couplers have long been used as passive optical components being able to combine or split SISO (single-input single-output) data transmission from optical fibers. Our results show by the obtained measured impulse responses together with the simulated BER performance that optical couplers are well suited for the optical MIMO transmission despite their insertion losses and asymmetries. Comparing the different couplers those which maintain the different optical mode groups support the MIMO transmission more efficiently.

1 Introduction

In the recent past the concept of MIMO (multiple input multiple output) transmission [1,2] over multimode fibers has attracted increasing interest in the optical fiber transmission community, targeting at increased fiber capacity [3,4]. The fiber capacity of a multimode fiber is limited by the modal dispersion compared to single-mode transmission where no modal dispersion except for polarization exists.

In MIMO transmission dispersion can be used to outperform the SISO transmission from an information theoretic point of view leading to higher fiber capacities and under practical circumstances to lower bit-error probabilities. The description of the optical MIMO channel has attracted attention and reached a state of maturity [3,5,6]. However, the realization of the optical MIMO channel requires substantial further research [7,8].

Against this background, the novel contribution of this paper is the use of optical couplers within a 1,4 km multimode (2×2) MIMO testbed. Based on the channel measurements, the different propagation paths within the MIMO system are described. To-

gether with the appropriate MIMO modeling and the corresponding signal processing (e. g. singular value decomposition), the efficiency of different optical couplers in MIMO communication is elaborated.

The remaining part of this contribution is organized as follows: Section 2 reviews the optical MIMO basics. Practical issues of optical MIMO including the use of optical couplers are introduced and discussed in section 3. The performance criteria used to evaluate the different optical couplers are introduced in section 4, while associated performance results are presented and interpreted in section 5. Finally, section 6 provides our concluding remarks¹.

2 Optical MIMO

An optical MIMO system can be formed by feeding different sources of light into the fiber, which support different optical modes. Theoretically, it can be done by using two single mode fibers as shown in Fig. 1. The different sources of light lead to different

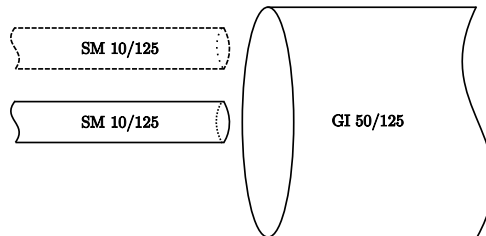


Figure 1: Transmitter side configuration with center and offset light launch condition

power distribution patterns at the fiber end depending on the transmitter side light launch conditions. Fig. 2 highlights the measured mean power distribution pattern at the end of a 1,4 km multimode fibre. Together with the appropriate receiver side spatial configurations, i. e. spot and ring filter (see Fig. 3), the electrical MIMO channel can be formed. Fig. 3

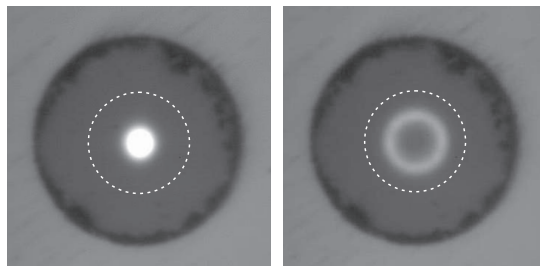


Figure 2: Measured mean power distribution pattern as a function of the light launch position (left: eccentricity $\delta = 0 \mu\text{m}$, right: eccentricity $\delta = 18 \mu\text{m}$); the dotted line represents the 50 μm core size.

illustrates the corresponding transmitter and receiver side configuration. Fig. 4 highlights the resulting electrical MIMO system model.

¹This paper was presented in parts at the International Conference on Optical Communication Systems (OPTICS) [9] as well as at the 15th ITG-Fachtagung Photonische Netze [10].

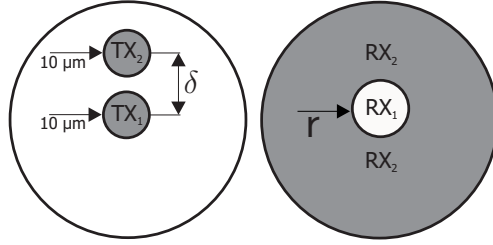


Figure 3: Forming the optical MIMO channel (left: light launch positions at the transmitter side with a given eccentricity δ , right: spatial configuration at the receiver side as a function of the mask diameter r)

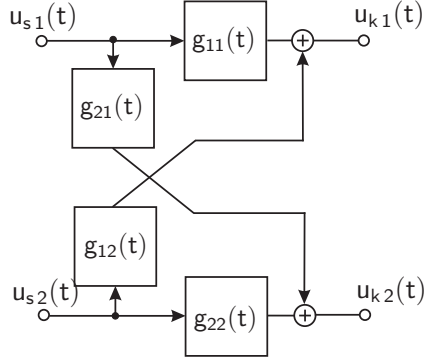


Figure 4: Electrical MIMO system model (example: $n = 2$)

Investigations in [11] have shown that an eccentricity of $\delta = 10 \mu\text{m}$ and a mask diameter of $r = 15 \mu\text{m}$ was found to be beneficial for minimizing the overall BER at a fixed data rate. However technologically an eccentricity of $\delta = 10 \mu\text{m}$ cannot be realized with two single mode fibres with a core size of $10 \mu\text{m}$ each. Therefore other transmitter side light launch conditions are in the focus of interest.

3 Practical Issues of Optical MIMO

A possible solution for feeding different sources of light in parallel in the fibre can be provided by optical couplers. In this section, various optical couplers are analyzed for their suitability in optical MIMO transmission systems (see Fig. 5). The focus within this section is on the transmitter side.

It is well known that optical couplers may show a very mode selective behavior [12]. In general this behavior depends on the fabrication technique [13]. Although the term 'mode selectivity' usually referred to the unwanted coupling ratio's dependency on the launching conditions we can make use of this parameter to control or better to maintain the mode groups within such a device.

Fig. 6–9 show the measured mean power distribution patterns at the fibre end when using different couplers at the transmitter side for feeding different sources of light into the fibre. The obtained intensity patterns are neither normalized nor related to each other. However, a good insight into the spatial mode structure is obtained.

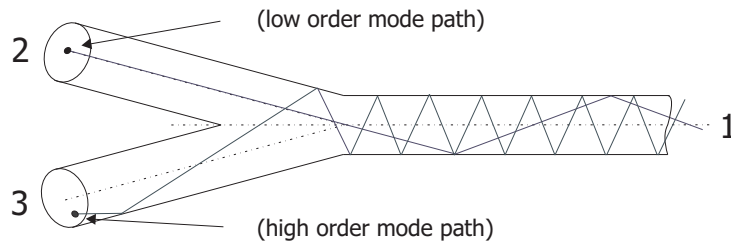


Figure 5: Transmitter side coupler for launching different sources of light into the MMF

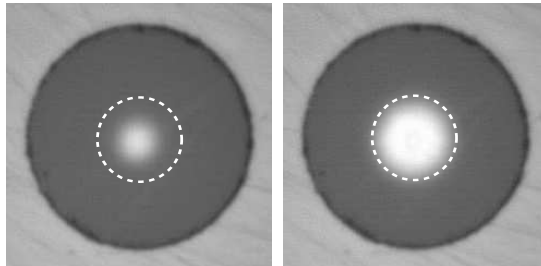


Figure 6: Measured mean power distribution pattern when using the symmetric fusion coupler (SFC) at the transmitter side (left: center light launch condition; right: off-center light launch condition, $\delta = 11\mu\text{m}$); the dotted line represents the $50\mu\text{m}$ core size.

Due to its inherent coupling mechanism the so called surface or evanescent field couplers, e.g. the fusion couplers start to couple light into the neighbor waveguide with the high order modes first. The strength of this behavior can be controlled by the degree of fusion. Therefore, the fusion coupler with the asymmetric coupling ratio which is realized by applying a low degree of fusion can easily split mode groups into high and low orders or combine them as can be seen when comparing Fig. 6 and 7. Unfortunately these asymmetric fusion couplers give also rise to very asymmetric MIMO channels which is caused by their coupling ratio (see Tab. 1). The coupling ratio a_{cr} can be obtained from the insertion losses a_{12} and a_{13} and results in

$$a_{\text{cr}} = |a_{13} - a_{12}| . \quad (1)$$

Table 1: Parameters of the transmitter-side couplers measured with restricted mode launch conditions as specified in Fig. 6–9 (in dB)

	SFC	AFC	PC	MC
excess loss a_e	2,3	2,5	3,2	3,8
coupling ratio a_{cr}	2,0	7,8	0,7	1,4

On the other hand 'butt-end' or end face couplers are usually considered to be less mode selective which is not true in general as can be seen from both Fig. 8 and Fig. 9.

Here the polished coupler shows strong support of the fundamental mode but it mixes several high order mode groups. Since it is all but impossible to polish the two fiber branches symmetrically and the optical modes respond very sensitive to these geomet-

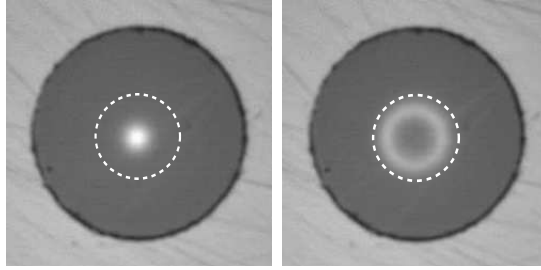


Figure 7: Measured mean power distribution pattern when using the asymmetric fusion coupler (AFC) at the transmitter side (left: center light launch condition; right: off-center light launch condition, $\delta = 15\mu\text{m}$); the dotted line represents the $50\mu\text{m}$ core size.

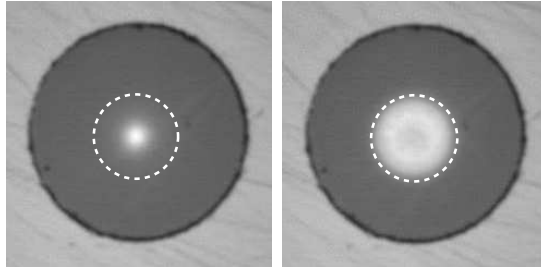


Figure 8: Measured mean power distribution pattern when using the polished coupler (PC) at the transmitter side (left: center light launch condition; right: high order mode path, $\delta = 0\mu\text{m}$); the dotted line represents the $50\mu\text{m}$ core size.

rical distortions the polished couplers show more or less mode selective behavior, too. Compared to fusion couplers they have the disadvantage of generally higher excess losses (see Tab. 1). The same holds true for couplers using micro optical parts, e.g. the mirror coupler. However, they may offer better mode control due to the easy access to the expanded optical fields. Fig. 9 shows qualitatively that the high order mode group is better maintained in comparison to the polished coupler in Fig. 8. In summary the three main parameters of couplers depend on fabrication techniques as indicated in Fig. 10.

Now, all impulse responses have been measured as described in [14] and [15] (see Fig. 11).

In order to exclude the impact of the different excess losses of the couplers (see Tab. 1) which can be related to fabrication deficiencies the overall powers at output 1 (Fig. 5) were equalized.

Though the power is equalized it spreads across the different mode groups supported by the respective couplers. Therefore different couplers will produce differing MIMO channels. Comparing $g_{22}(t)$ in Fig. 12 to 15 the power spreading across the high order modes is emphasized. This is expected since the number of excited mode groups increases with the radial launching offset δ . However the different couplers may further increase this number by mode coupling. The lowest spreading shows the asymmetric fusion coupler with four mode groups whereas the polished coupler produces eight mode groups. Likewise the fundamental mode is mainly supported by both the asymmetric fusion and the polished couplers whereas the other couplers also excite the next higher mode. The disadvantage

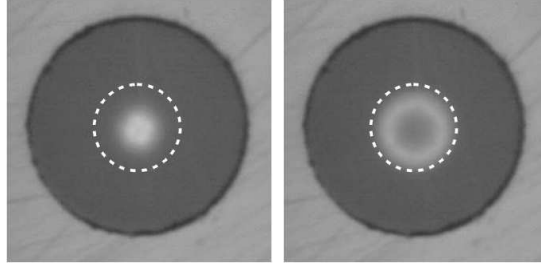


Figure 9: Measured mean power distribution pattern when using the mirror coupler (MC) at the transmitter side (left: center light launch condition; right: off-center light launch condition, $\delta = 10\mu\text{m}$); the dotted line represents the $50\mu\text{m}$ core size.

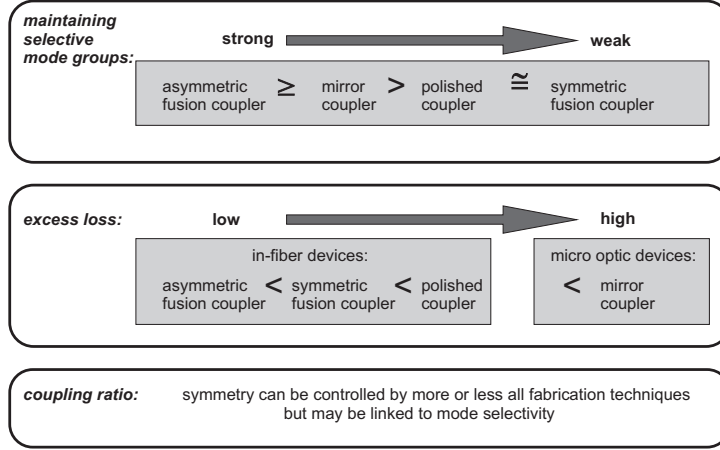


Figure 10: Relationship between fabrication techniques and coupler parameters.

of the unequal coupling ratio of an asymmetric fusion coupler compared to a symmetric one is not as evident as expected which can be seen from $g_{22}(t)$ in Fig. 12 and 13. This is caused by the restricted mode launching conditions and how the coupler maintains certain modes.

4 Performance Criteria

For the performance evaluation of the different MIMO configurations, coherent transmission and detection is assumed together with the modulation format QAM (quadrature amplitude modulation) per MIMO transmission mode. The block-oriented system for

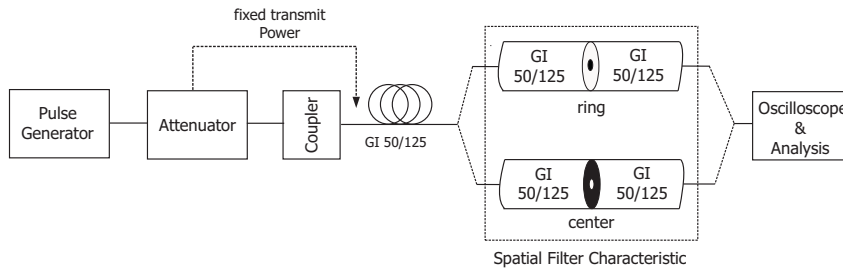


Figure 11: Measurement setup for measuring the MIMO specific impulse responses

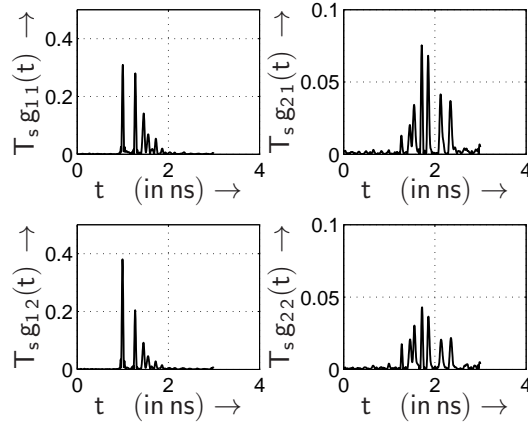


Figure 12: Measured electrical MIMO impulse responses with respect to the pulse frequency $f_T = 1/T_s = 5,00$ GHz at 1326 nm operating wavelength when using the symmetric fusion coupler at the transmitter side

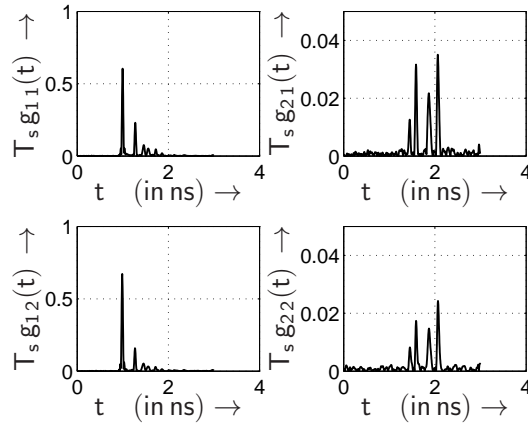


Figure 13: Measured electrical MIMO impulse responses with respect to the pulse frequency $f_T = 1/T_s = 5,00$ GHz at 1326 nm operating wavelength when using the asymmetric fusion coupler at the transmitter side

frequency selective channels is modeled by:

$$\mathbf{u} = \mathbf{H} \cdot \mathbf{c} + \mathbf{w} . \quad (2)$$

In (2), the transmitted signal vector \mathbf{c} is mapped by the channel matrix \mathbf{H} onto the received vector \mathbf{u} . Finally, the vector of the additive, white Gaussian noise (AWGN) is defined by \mathbf{w} [14, 16]. Details on the transmission model, which has been determined by channel measurements, are given in [14]. Singular-value decomposition (SVD) can now be used to transfer the whole MIMO system into independent, non-interfering layers exhibiting unequal gains per layer as highlighted in Fig. 16, where as a result weighted additive, white Gaussian noise (AWGN) channels appear. The data symbols at the time k , i.e. c_{1k} and c_{2k} are weighted by the positive square roots of the eigenvalues of the matrix $\mathbf{H}^H \mathbf{H}$, i.e. $\sqrt{\xi_{1k}}$ and $\sqrt{\xi_{2k}}$. Finally, some noise is added, i.e. w_{1k} and w_{2k} .

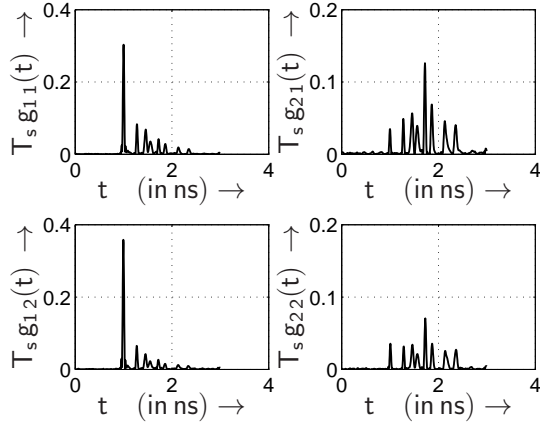


Figure 14: Measured electrical MIMO impulse responses with respect to the pulse frequency $f_T = 1/T_s = 5,00$ GHz at 1326 nm operating wavelength when using the polished coupler at the transmitter side

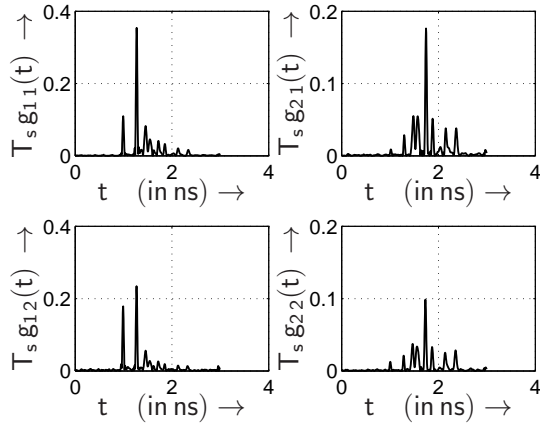


Figure 15: Measured electrical MIMO impulse responses with respect to the pulse frequency $f_T = 1/T_s = 5,00$ GHz at 1326 nm operating wavelength when using the mirror coupler at the transmitter side

5 Results

For comparing the different MIMO configurations, a fixed transmission bit rate is assumed. Furthermore, for numerical analysis it is assumed, that each optical input within the multimode fiber is fed by a system with identical mean properties with respect to transmit filter and pulse frequency $f_T = 1/T_s$. Rectangular pulses are used for transmit and receive filtering. For numerical assessment within this paper, the pulse frequency is chosen to be $f_T = 5,00$ GHz, the average transmit power is supposed to be $P_s = 1 \text{ V}^2$ – this equals 1 W at a linear and constant resistance of 1Ω – and as an external disturbance a white Gaussian noise with power spectral density N_0 is assumed [14]. Tab. 2 highlights the different transmission modes to be investigated when minimizing the overall BER.

In order to transmit at a fixed data rate while maintaining the best possible integrity, i. e. bit-error rate (BER), an appropriate number of MIMO layers has to be used, which depends on the specific QAM constellation size as well as the layer-specific weighting factors, i. e. $\sqrt{\xi_{1k}}$ and $\sqrt{\xi_{2k}}$.

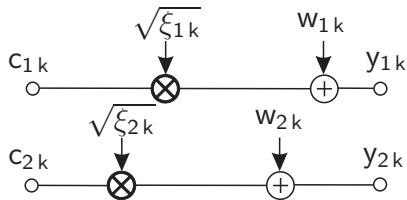


Figure 16: SVD-based layer-specific transmission model

Table 2: Parameters for bitloading: Investigated QAM transmission modes for fixed transmission bit rate

throughput	layer 1	layer 2
4 bit/s/Hz	16	0
4 bit/s/Hz	4	4

For a given MIMO configuration, i. e. the asymmetric fusion coupler at the transmitter side and the spatial filters at the receiver side, the corresponding BER performance is depicted in Fig. 17. As shown by the BER results, the achievable performance of the MIMO system is strongly affected by the number of bits transmitted per activated MIMO layer. Using SVD, the singular values are ordered in descending order. That's why only the strongest layers should be used for the data transmission with appropriate QAM modulation levels.

Fig. 18 shows the obtained BER performance when using the different transmitter side coupler configurations. As highlighted by the BER results, the asymmetric fusion coupler (AFC) shows the best performance among the investigated coupler configurations. Therein, unequal coupling ratio of an asymmetric fusion coupler seems to be highly beneficial when minimizing the overall BER.

6 Conclusion

In this work the use of optical couplers in a (2×2) MIMO testbed is studied and analyzed for a 1,4 km multimode MIMO channel. As shown by the obtained measured impulse responses as well as the simulated BER results, optical couplers are well suited for the optical MIMO transmission. As shown by the simulation results, couplers maintaining the different mode groups without additional mixing seem to be beneficial when minimizing the overall BER.

References

- [1] V. Kühn. *Wireless Communications over MIMO Channels – Applications to CDMA and Multiple Antenna Systems*. Wiley, Chichester, 2006.

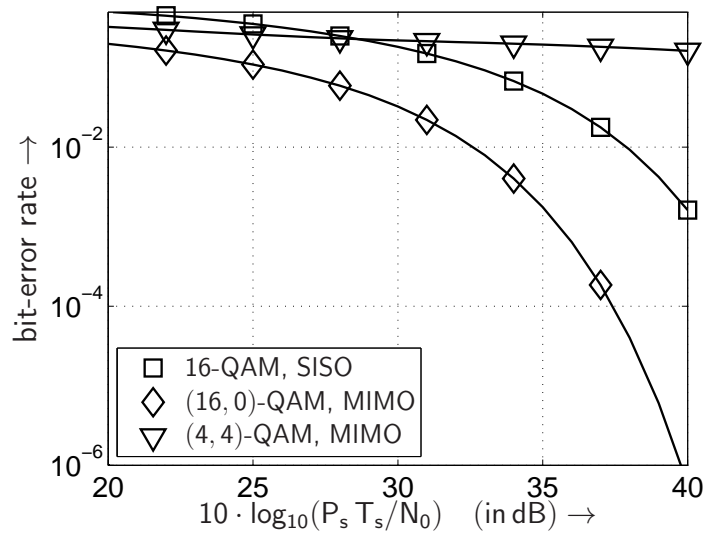


Figure 17: BER performance at 1326 nm operating wavelength when using the asymmetric fusion coupler at the transmitter side, the transmission modes introduced in Tab. 2 and transmitting 4 bit/s/Hz over frequency selective optical MIMO channels

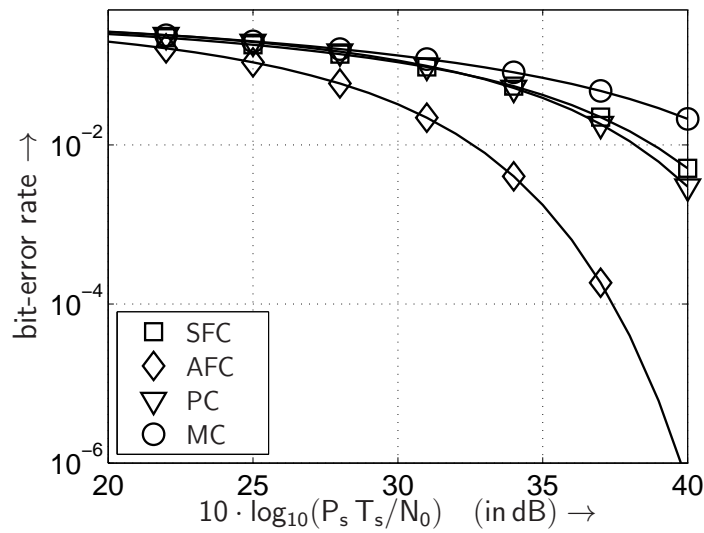


Figure 18: Coupler specific BER performance at 1326 nm operating wavelength when using the (16, 0) QAM transmission mode

- [2] G. J. Foschini. Layered Space-Time Architecture for Wireless Communication in a Fading Environment when using Multiple Antennas. *Bell Labs Technical Journal*, 1(2):41–59, 1996.
- [3] A. C. Singer, N. R. Shanbhag, and Hyeon-Min Bae. Electronic Dispersion Compensation– An Overview of Optical Communications Systems. *IEEE Signal Processing Magazine*, 25(6):110 – 130, 2008.
- [4] S. Aust, A. Ahrens, and S. Lochmann. Channel-Encoded and SVD-assisted MIMO Multimode Transmission Schemes with Iterative Detection. In *International Conference on Optical Communication Systems (OPTICS)*, pages 353–360, Rom (Italy), July 24-27 2012.
- [5] R. C. J. Hsu, A. Tarighat, A. Shah, A. H. Sayed, and B. Jalali. Capacity Enhancement in Coherent Optical MIMO (COMIMO) Multimode Fiber Links. *IEEE Communications Letters*, 10(3):195–197, 2006.
- [6] H. Bülow, H. Al-Hashimi, and B. Schmauss. Coherent Multimode-Fiber MIMO Transmission with Spatial Constellation Modulation. In *European Conference and Exhibition on Optical Communication (ECOC)*, Geneva, Switzerland, September 18-22 2011.
- [7] S. Schöllmann and W. Rosenkranz. Experimental Equalization of Crosstalk in a 2 x 2 MIMO System Based on Mode Group Diversity Multiplexing in MMF Systems @ 10.7 Gb/s. In *33rd European Conference and Exhibition on Optical Communication (ECOC)*, Berlin, September 2007.
- [8] S. Schöllmann, N. Schrammar, and W. Rosenkranz. Experimental Realisation of 3 x 3 MIMO System with Mode Group Diversity Multiplexing Limited by Modal Noise. In *Optical Fiber Communication Conference (OFC)*, San Diego, California, February 2008.
- [9] A. Ahrens and S. Lochmann. Optical Couplers in Multimode MIMO Transmission Systems: Measurement Results and Performance Analysis. In *International Conference on Optical Communication Systems (OPTICS)*, pages 398–403, Reykjavik (Iceland), 29.–31. July 2013.
- [10] A. Sandmann, A. Ahrens, and S. Lochmann. Experimental Description of Multimode MIMO Channels utilizing Optical Couplers. In *15. ITG-Fachtagung Photonische Netze – ITG-Fachbericht Band 248*, pages 125–130, Leipzig (Germany), 05.–06. May 2014.
- [11] A. Ahrens, J. Pankow, S. Aust, and S. Lochmann. Optical MIMO Multimode Fiber Links: Channel Measurements and System Performance Analysis. In *International Conference on Optical Communication Systems (OPTICS)*, pages 128–132, Seville (Spain), 18.–21. July 2011.

- [12] S. Lochmann and M. Becker. Cover Photo of the Journal. *Nachrichtentechnik, Elektronik*, 33(11), 1983.
- [13] S. Lochmann, W. Scheel, J. Labs, and T. Wallstein. Passive Optical Splitters (in German). *Nachrichtentechnik, Elektronik*, 33(11):444–448, 1983.
- [14] J. Pankow, S. Aust, S. Lochmann, and A. Ahrens. Modulation-Mode Assignment in SVD-assisted Optical MIMO Multimode Fiber Links. In *15th International Conference on Optical Network Design and Modeling (ONDM)*, Bologna (Italy), 8.-10. February 2011.
- [15] A. Ahrens, S. Schröder, and S. Lochmann. Dispersion Analysis within a Measured 1,4 km MIMO Multimode Channel. In *International Conference on Optical Communication Systems (OPTICS)*, pages 391–397, Reykjavik (Iceland), 29.–31. July 2013.
- [16] G. G. Raleigh and J. M. Cioffi. Spatio-Temporal Coding for Wireless Communication. *IEEE Transactions on Communications*, 46(3):357–366, March 1998.